signals (C=O, C-4, and C-1) decay very slowly; the methyl carbon signal decays more rapidly; and the aromatic CH and methylene carbon signals decay the fastest. The dipolar modulation is particularly evident in **5** for the protonated aromatic resonances C-2,6 and C-3,5. The rotational modulation at $2/\omega_r$ (about 560 μs) is also evident. The same phenomena are evident in Figure 8 for **1**. The rotational modulation at $1/\omega_r$ (about 250 μs) is clearly evident. Previous work[6,11,12,16] and Figures 7 and 8 show that a high S/N ratio is usually required to detect the modulation effects. Plots of the signal intensities in **1** as a function of t_1 appear for the nonprotonated ring carbons in Figure 9a, for the protonated ring carbons in Figure 9b, for the methine carbons in Figure 9c, and for the methyl carbons in Figure 9d. For each of the four resolved carbon signals, the decay of the signal amplitude is clearly modulated. The rotational modulation at $2/\omega_r$ is clearly evident in Figures 9a and 9c. The dipolar modulation involving both positive and negative signals is evident in Figures 9a-c. As expected, the CH carbons exhibit the strongest dipolar modulation. The data shown in Figure 8 and the decay patterns shown in Figures 9a-c adequately demonstrate the well-documented dipolar modulation effects[6,11,12,16] and provide approximate dipolar coupling constants. The decay patterns in Figures 9a-d represent cross sections parallel to the t_1 axis of constant F_2, and therefore constitute a free induction decay in t_2. Fourier transformation of these data gives a dipolar spectrum.[6,11,12,16] Finally, we note that the data in Tables I and II are not relevant to experiments in which spin diffusion among the protons during t_1 is suppressed.[16]

Conclusions

Both conventional cross polarization and dipolar dephasing studies at a variety of contact or delay times, respectively, provide information on the magnitude of the $^{13}C-^{1}H$ dipole-dipole interactions. Such information greatly facilitates signal assignments[1,8-10,14,25,26] and provides valuable insights into the proton environment and into the extent of motional freedom in the solid. The application of these techniques to complex solids that cannot be adequately characterized by other methods has been and should continue to be very useful. For example, these results and others[8,9,11-14,17] strongly suggest that spectra obtained under conventional conditions and under a 55-μs suspension of the proton locking field will reveal, respectively, all the carbon atoms and the somewhat attenuated signals of only methyl and nonprotonated carbon atoms. Slightly shorter dephasing periods also suffice in some instances, depending upon the degree of motional freedom present in the sample.

Acknowledgment. We are pleased to acknowledge very helpful discussions with Drs. Kurt W. Zilm and Michael A. Wilson. Support for this work was provided by the Office of Energy Research, U. S. Department of Energy, under Contract No. DE-AS02-78ER05006.

Registry No. 1, 26886-05-5; **2**, 1498-96-0; **3**, 538-39-6; **4**, 6922-60-7; **5**, 4919-33-9; **6**, 121-46-0; **7**, 14233-37-5; **8**, 691-64-5; **9**, 1012-72-2; **10**, 128-37-0; **11**, 626-51-7.

Acetylene and Ethylene Complexes of Gold Atoms: Matrix Isolation ESR Study

Paul H. Kasai

Contribution from IBM Instruments, Inc., Danbury, Connecticut 06810. *Received April 15, 1983*

Abstract: Gold atoms were trapped in argon matrices containing ethylene or acetylene and were examined by electron spin resonance spectroscopy. The spectral analyses revealed formations of π-coordinated gold(0)-mono(ethylene), gold(0)-mono(acetylene), and gold(0)-bis(ethylene) complexes and, in matrices of high acetylene concentration, gold(0)-acetylene adduct of the vinyl form. The **g** tensors and the Au-197 hyperfine coupling tensors of these compounds were determined and analyzed. The monoligand complexes, $Au(C_2H_4)$ and $Au(C_2H_2)$, are held primarily by the dative interaction between the filled d_{xy} orbital of the metal and the antibonding π_y^* orbital of the ligand. The semifilled orbital is an sp-hybridized orbital of the metal pointing away from the ligand. In bis(ethylene)gold(0) the metal atom is flanked by two ligand molecules oriented parallel to each other. The complex is held by the dative interaction between the semifilled p_x orbital of the metal parallel to the ligands and the antibonding π_y^* orbitals of the ligands.

Metal atom chemistry in which vaporized metal atoms are trapped and allowed to react with molecules condensed at cryogenic temperature has been the subject of many recent reports.[1-5] Elucidation of the structure and the orbital property of complexes between transition-metal atoms and unsaturated organic molecules is of particular interest because of its relevance to organometallic syntheses and transition-metal catalysis. IR and UV-visible spectra of ethylene complexes of Cu, Ag, and Au atoms and acetylene complexes of Ni and Cu atoms have been analyzed by Ozin and his co-workers.[6-8]

Electron spin resonance (ESR) spectra of acetylene and ethylene complexes of Cu and Ag atoms generated in rare gas matrices have also been reported.[9] The ESR study showed that Cu atoms form both mono- and diligand complexes with either acetylene or ethylene. Structural features of these complexes have been elucidated as follows.

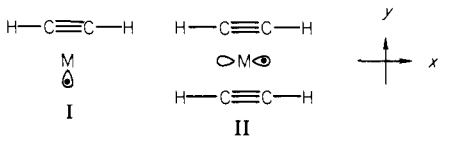

In structure I the unpaired electron is located in an sp_y orbital of the metal atom pointing away from the ligand, and in structure

(1) *Angew. Chem., Int. Ed. Engl.*, **1975**, *14*, 273, a collection of review articles on the subject.
(2) Moskovitz, M.; Ozin, G. A. "Cryochemistry"; Wiley: New York, 1976.
(3) Ozin, G. A. *Acc. Chem. Res.* **1977**, 10, 21.
(4) Moskovitz, M. *Acc. Chem. Res.* **1979**, *12*, 229.
(5) Klabunde, K. J. "Chemistry of Free Atoms and Particles; Academic Press: New York, 1980.
(6) Ozin, G. A.; Huber, H.; McIntosh, D. *Inorg. Chem.* **1977**, *16*, 3070.
(7) McIntosh, D.; Ozin, G. A. *J. Organomet. Chem.* **1976**, *121*, 127.
(8) Ozin, G. A.; McIntosh, D. F.; Power, W. J.; Messmer, R. P. *Inorg Chem.* **1981**, *20*, 1782.
(9) Kasai, P. H.; McLeod, D., Jr.; Watanabe, T. *J. Am. Chem Soc.* **1980**, *102*, 179.

0002-7863/83/1505-6704$01.50/0

II it is located in the metal p_x orbital parallel to the ligands. Both types of complexes are formed by the dative interactions of the Dewar–Chatt–Duncanson scheme;[10,11] possible modes of interactions are donation from the filled π_y orbital(s) of the ligand(s) into the vacant s and p_y orbitals of the metal atom, donation from the filled d_{xy} orbital of the metal into the vacant π_y^* orbital(s), and, in the latter case, donation from the semifilled p_x orbital of the metal into the π_y^* orbitals.

Ag atoms, in contrast, were found to form a bona fide complex with the bis(ethylene) system (structure II), but only "pseudocomplexes" of weak interaction with monoethylene, monoacetylene, and diacetylene species in the matrices. In the special case of Ag atoms allowed to react with acetylene in the vapor phase, a silver–acetylene adduct having the vinyl form III was generated. The difference in the complexing behaviors of the

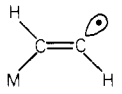

III

Cu and Ag atoms was attributed to the difference in the energy levels of the Cu 3d and Ag 4d orbitals.

Most intriguingly the energy level of the Au 5d orbital is midway between those of the Cu 3d and Ag 4d orbitals.[12] The present paper reports on ESR examination of complexes generated when Au atoms and ethylene or acetylene molecules were cocondensed in argon matrices. The study revealed that Au atoms form both mono- and diligand complexes (of structures I and II) with ethylene. The gold/acetylene/argon system also showed two sets of ESR signals due to gold(0)–acetylene complexes. One of these is readily recognized as that of the monoligand complex of structure I. The spectral pattern of the second set, however, suggests that it be assigned to a gold–acetylene adduct of structure III, and not to the diligand complex.

Experimental Section

An X-band ESR spectrometer–liquid helium cryostat system that would allow trapping of vaporized atoms in a rare gas matrix and examination of the resulting matrix by ESR has already been described.[13] In the present series of experiments Au atoms were vaporized from a resistively heated (~1500 °C) tantalum cell and were condensed in argon matrices containing ethylene or acetylene. The concentrations of ethylene and acetylene were varied from 1 to 10 mol % and that of the metal atoms was maintained at 0.1 mol %. Because of the wetting and alloying property of molten gold, gold pellets were placed in an alumina tube, capped with a molybdenum plug, and then placed in the tantalum cell. The gold vapor effused through an opening drilled through the Ta and alumina walls.

The cryostat is equipped with a side quartz window through which the matrix can be irradiated. For irradiation a high-pressure Xe–Hg arc lamp (Oriel 1 kW) was used together with a set of sharp cut-off filters.

Deuterated ethylene and acetylene, C_2D_4 and C_2D_2, ^{13}C-enriched ethylene, $H_2{}^{13}C{=}CH_2$, and ^{13}C enriched deuterated acetylene, $^{13}C_2D_2$, were all obtained from Merck Chemical Division.

All the ESR spectra reported here were recorded while the matrices were maintained at ~4 K. The spectrometer frequency locked to the sample cavity was 9.425 GHz.

Spectra and Assignments

Gold Atom–Ethylene Complexes. The ESR spectrum of Au atoms isolated in an argon matrix had been studied earlier. The spectrum is a sharp, widely spaced quartet due to an isotropic hf (hyperfine) interaction between the unpaired electron in the 6s orbital and the ^{197}Au nucleus (natural abundance = 100%, $I = {}^3/_2$, $\mu = 0.1439\beta_n$). The hf coupling constant of Au atoms in an argon matrix is 3.1379 GHz (1120 G).[14]

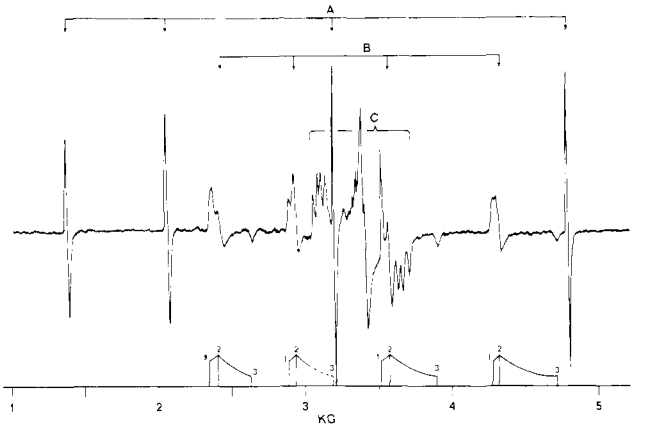

Figure 1. ESR spectrum of an argon matrix containing Au and ethylene (C_2H_4; 10%). The bar graph at the bottom indicates the analysis of the B signals; the numerals indicate the resonance positions when the field is along the corresponding principal axis.

The ESR spectrum observed from an argon matrix containing Au and ethylene (10%) is shown in Figure 1. Three sets of signals, A, B, and C, can be recognized as indicated. The signals A are due to isolated Au atoms. When the ethylene concentration was lowered to 3.3%, the intensities of signals B and C decreased by factors of ~3 and ~9, respectively. The signals B and C are thus assigned to gold(0)–mono(ethylene), and gold(0)–bis(ethylene) complexes, respectively. No discernible change was noted in either of these signals when the experiment was repeated with perdeuterioethylene, C_2D_4.

The quartet pattern of the B signals must arise from the hf interaction with the Au nucleus; further splittings of each component indicated in the figure are due to orthorhombicities of the **g** tensor and/or the hf coupling tensor. The observed resonance positions of the B signals are given in Table I. The spacings of these signals are so large that they cannot be analyzed by the usual second-order solution of a spin Hamiltonian.

When the principal axes of the **g** tensor and the hf coupling tensor coincide and the z axis lies parallel to the external field, a spin Hamiltonian of a radical with $S = {}^1/_2$ and one magnetic nucleus can be written as follows.

$$\mathcal{H}_{spin} = g_z\beta HS_z + AS_zI_z + BS_xI_x + CS_yI_y \qquad (1)$$

Here A, B, and C are the diagonal elements of the principal hf coupling tensor. It has been shown that the secular determinant derived from Hamiltonian 1 can be expanded exactly using the continued fraction technique,[15] and the resonance field $H_z(m)$ of a hf component ($m_I = m$) can be given accurately by the following "continued expression":[9]

$$\mathcal{H}_z(m) = H_z^0 - mA' - F - G \qquad (2)$$

where

$$F = \frac{Q^2[I(I+1) - m(m+1)]}{H_z(m) + (m + {}^1/_2)A' + F}$$

$$G = \frac{Q^2[I(I+1) - m(m-1)]}{H_z(m) + (m - {}^1/_2)A' + G}$$

and $H_z^0 = h\nu/g_z\beta$, $A' = A/g_z\beta$, $B' = B/g_x\beta$, $C' = C/g_y\beta$ and $Q = (1/4g_z)(B'g_x + C'g_y)$. The expressions for the resonance positions $H_x(m)$, and $H_y(m)$ can be generated by appropriate permutations of (g_x, g_y, g_z) and (A', B', C') in eq 2.

From the observed resonance positions of the $m_I = \pm{}^3/_2$ components and the set of equations 2 developed for $H_x(m)$, $H_y(m)$, and $H_z(m)$, the consistent set of **g** values and hf constants can be readily determined through a computer-assisted iteration

(10) Dewar, M. J. S. *Bull. Soc. Chim. Fr.* **1951**, *18*, C79.
(11) Chatt, J.; Duncanson, L. A. *J. Chem. Soc.* **1953**, 2939.
(12) Moore, C. E. *Natl. Bur. Stand. (U.S.), Circ.* **1949**, *1* (No. 467); **1952**, *2* (No. 467); **1958**, *3* (No. 467).
(13) Kasai, P. H., *Acc. Chem Res.* **1971**, *4*, 329.
(14) Kasai, P. H., McLeod, D., Jr. *J. Chem. Phys. 1971*, *55*, 1566.
(15) See, for example, Strandberg, M. W. "Microwave Spectroscopy"; Methuen: London, 1954, p 11.

Table I. Observed Resonance Positions of $Au(C_2H_4)$ and $Au(C_2H_2)$[a]

complex	axis	hyperfine component (m_I)[b] $+^3/_2$	$+^1/_2$	$-^1/_2$	$-^3/_2$
$Au(C_2H_4)$	1	2350	2876	3514	4287
	2	2412	2926	3565	4328
	3	2633	(3193)	3897	4728
$Au(C_2H_2)$	1	2245	2800	3466	4285
	2	2295	2825	(3498)	4315
	3	2445	(3009)	(3726)	4595

[a] Given in G; accuracy ±3 G; microwave frequency 9.425 GHz. [b] When the signal is masked by others, the computed value is given in parentheses.

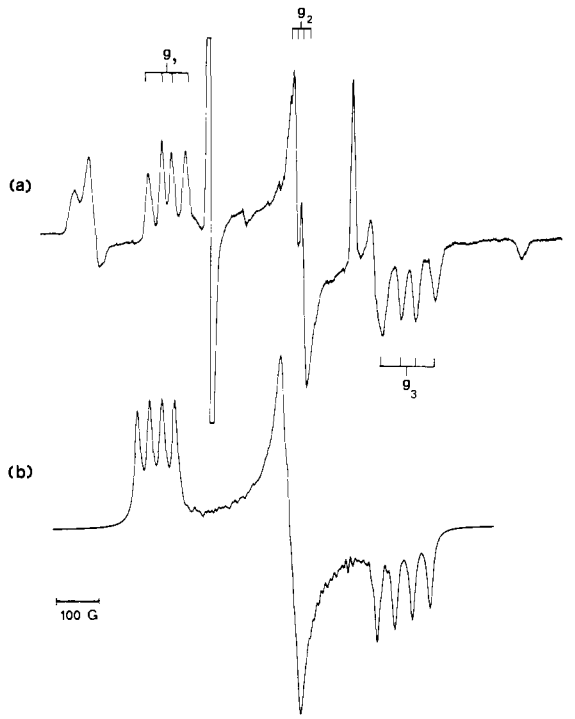

Figure 2. (a) C signal region (of Figure 1) shown in an expanded scale. (b) Simulated spectrum based upon the parameters given in the text.

process. The **g** tensor and the ^{197}Au hf coupling tensor of the gold(0)–mono(ethylene) complex were thus determined as follows.

$$g_1 = 1.978\ (2) \qquad g_2 = 1.946\ (2) \qquad g_3 = 1.782\ (2)$$

$$A_1 = 1.772\ (2) \qquad A_2 = 1.725\ (2) \qquad A_3 = 1.726\ (2)\ \text{GHz}$$

The resonance positions of all the B signals computed from eq 2 based upon these tensors are all within the experimental uncertainty (±3 G) of the observed values. The large, essentially isotropic hf interaction with the Au nucleus and the absence of hf structure due to protons are consistent with structure I.

The C signals assigned to gold(0)–bis(ethylene) complex is shown expanded in Figure 2a. They overlap with the $m_I = -^1/_2$ component of the Au atom spectrum, and the $m_I = \pm^1/_2$ components of the gold(0)–mono(ethylene) spectrum. The C signals themselves are recognized as the powder pattern of a system having a highly anisotropic **g** tensor and small hf structures (a quartet due to ^{197}Au) resolved along two principal axes of the **g** tensor.[16] These signals can be analyzed by the usual second-order solution of a spin Hamiltonian. By use of the method of computer simulation (of the ESR spectrum of randomly oriented radicals),[17] the **g** tensor and the ^{197}Au hf coupling tensor of the gold(0)–bis(ethylene) complex were determined as follows.

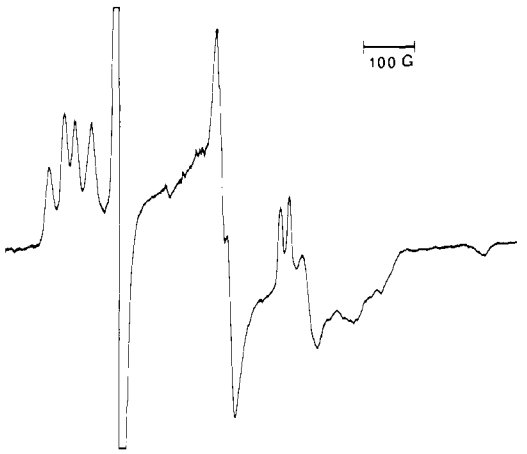

Figure 3. C signal region of the ESR spectrum observed from the $Au/H_2{}^{13}C{=}CH_2(6\%)/Ar$ system.

$$g_1 = 2.180\ (2) \qquad g_2 = 1.984\ (2) \qquad g_3 = 1.846\ (2)$$

$$A_1 = 28.3 \pm 0.5 \qquad A_2 = 10.0 \pm 2.0 \qquad A_3 = 40.0 \pm 0.5\ \text{G}$$

Figure 2b is a computer-simulated spectrum based on these parameters and a Lorentzian line shape with the line width of 8 G. The small, highly anisotropic ^{197}Au coupling tensor, the absence of hf structure due to protons, and the highly anisotropic **g** tensor are all consistent with structure II.

The hf structures resolved along the g_1 and g_3 regions are such that the outer spacings are larger than the inner spacing. The splitting observed at the g_2 region also suggests a partially resolved hf structure of uneven spacing. These features are expected from a nuclear quadrupole interaction.[18] Attempts to reproduce these features in the simulated spectrum by incorporating the second-order solution of the quadrupole interaction term have not been successful, however.

Figure 3 shows the C signal region of the ESR spectrum observed when the matrix was prepared using $H_2{}^{13}C{=}CH_2$, where only one of the carbon atoms was enriched (90%) with the ^{13}C nucleus. The ^{13}C substitution splits the g_1 peak of the gold(0)–mono(ethylene) spectrum, broadens the g_3 section of the gold(0)–bis(ethylene) spectrum, but leaves the remaining signals essentially unaffected. Through computer simulation it was determined that the broadening at g_3 of the bis(ethylene) complex resulted from "1:2:1" splitting (with the spacing of ~20 G) of the original quartet. The ^{13}C hf coupling tensors of these complexes were thus determined as follows.

For $Au(C_2H_4)_1$

$$A_1 = 18\ (1) \qquad A_2 = 0\ (3) \qquad A_3 = 0\ (3)\ \text{G}$$

For $Au(C_2H_4)_2$

$$A_1 = 0\ (3) \qquad A_2 = 0\ (3) \qquad A_3 = 20\ (1)\ \text{G}$$

We should further note the ^{13}C hf structure substantiates the presence of two equivalent ethylene molecules in the latter complex.

When argon matrices showing the signals A, B, and C discussed above were irradiated with visible light ($\lambda > 4000$ Å) for 10 min, the B signals disappeared completely, while the other signals remained unaltered.

Gold Atom–Acetylene Complexes. The ESR spectrum observed from an argon matrix containing Au and acetylene (10%) is shown in Figure 4. Three sets of signals, A, B, and C, are again recognized. The signals A are due to isolated Au atoms. When the acetylene concentration was lowered to 5%, the intensities of the signals B and C decreased by factors of ~2 and ~4, respectively.

The similarity of the B signals to those in Figure 1 is striking.

(16) See, for example, Atkins, P. W., Symons, M. C. R. "The Structure of Inorganic Radicals"; Elsevier: Amsterdam, 1967.

(17) The simulation program used is described in Kasai, P. H. *J. Am. Chem. Soc.* **1972**, *94*, 5950.

(18) Bleaney, B. *Philos. Mag.* **1951**, *42*, 441.

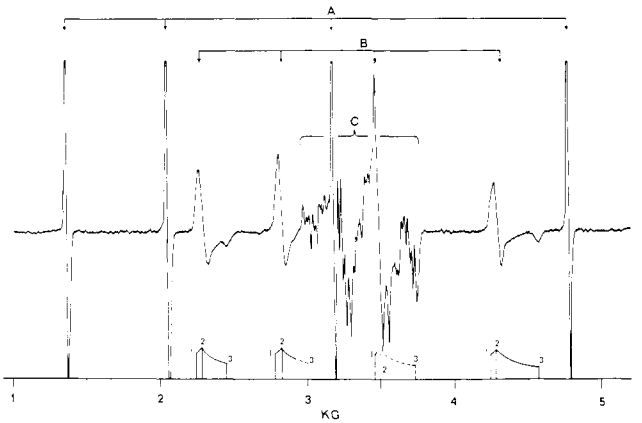

Figure 4. ESR spectrum of an argon matrix containing Au and acetylene (C_2H_2; 10%). The bar graph at the bottom indicates the analysis of the B signals; the numerals indicate the resonance positions when the field is along the corresponding principal axis.

The B signals are hence assigned to gold(0)–mono(acetylene) complex of structure I. No discernible change was noted in these signals when the experiment was repeated with perdeuterioacetylene, C_2D_2. The observed resonance positions of the monoacetylene complex are given in Table I. By the method based on eq 2 and described thereafter, the **g** tensor and the ^{197}Au hf coupling tensor of the gold(0)–monoacetylene complex were determined as follows.

$$g_1 = 2.003\ (2) \qquad g_2 = 1.977\ (2) \qquad g_3 = 1.856\ (2)$$

$$A_1 = 1.888\ (2) \qquad A_2 = 1.845\ (2) \qquad A_3 = 1.844\ (2)\ \text{GHz}$$

The resonance positions of all the B signals computed from eq 2 based upon these tensors are all within the experimental uncertainty (±3 G) of the observed values.

The C signals observed from the Au/C_2H_2 (10%)/Ar system is shown expanded in Figure 5a and is compared with the C signals oberved from the Au/C_2D_2 (10%)/Ar system, Figure 5b. The broad quartet pattern resolved in Figure 5b with the successive spacings of ~220 G must be ascribed to the hf structure due to ^{197}Au. The weak signals interspaced within the quartet are attributed to the forbidden transitions caused by a nuclear quadrupole interaction. The C signals observed here are thus significantly different from those of bis(ethylene)gold(0); in particular (1) they exhibit large hf structures due to protons, (2) the ^{197}Au hf coupling tensor is larger by an order of magnitude and is quite isotropic, and (3) the anisotropy of the **g** tensor is small.

As stated earlier the ESR spectrum of bis(acetylene)copper(0) is known.[9] Consistently with structure II it is characterized by a small, highly anisotropic hf coupling tensor with the Cu nucleus, and rather large hf interactions (28 G) with four equivalent protons. A precise analysis of the C signals in Figure 5 is made difficult by the presence of signals due to forbidden transitions and those due to gold atoms and the gold(0)–mono(acetylene) complex. However, the ^{197}Au hf coupling tensor revealed in Figure 5b is clearly too large and too isotropic to be that arising from the unpaired electron density in the Au $6p_x$ orbital. Also the proton hf structures recognizable through comparison of Figure 5, parts a and b, suggest a doublet-of-doublet pattern expected from hf couplings with two nonequivalent protons. The spectrum is therefore assigned to an gold–acetylene adduct of the vinyl form.

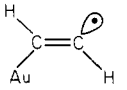

A further substantiation to this assignment was obtained when the matrix was prepared using ^{13}C enriched (90%) perdeuterioacetylene, $^{13}C_2D_2$ (Figure 6). As indicated in the figure most of the signals can be reconciled with a quartet-of-doublet pattern with the respective spacings of ~220 and ~80 G; the remaining signals are presumably caused by the nuclear quadrupole effect.

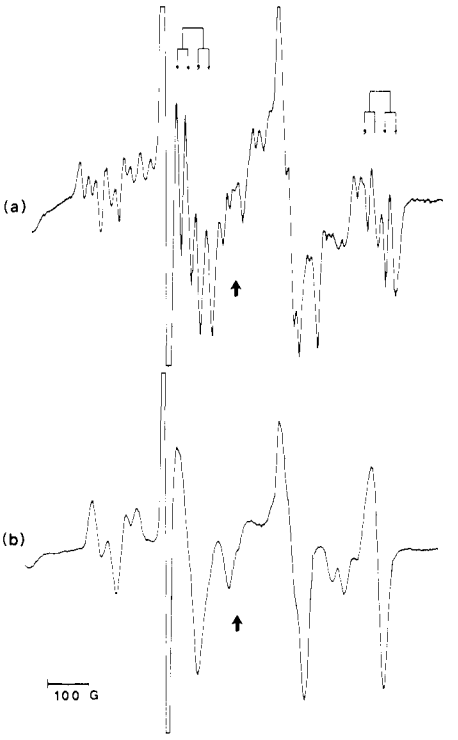

Figure 5. (a) C signal region (of Figure 4) shown in an expanded scale. (b) C signal region observed from the Au/C_2D_2(10%)/Ar system. Doublet-of-doublet patterns due to two nonequivalent protons are recognized in some components of the former as indicated. The solid arrows indicate the positions corresponding to $g = 2.002$.

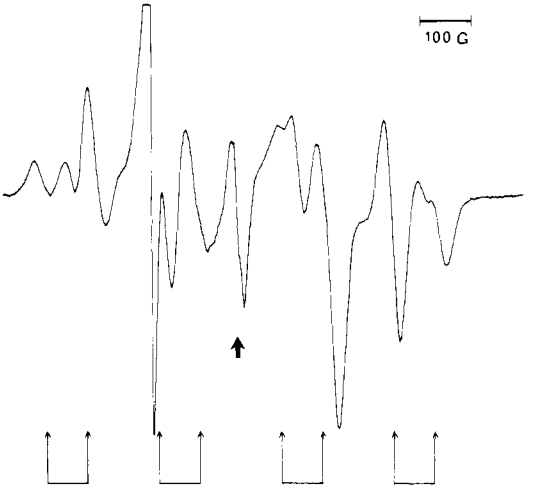

Figure 6. C signal region observed from the $Au/^{13}C_2D_2$ (10%)/Ar system. A quartet-of-doublet pattern can be recognized as indicated. The solid arrow indicates the position corresponding to $g = 2.002$.

The **g** tensor and the hf coupling tensors of the gold–acetylene adduct, all of which appeared essentially isotropic, were determined as follows.

$$g = 2.002 \pm 0.006$$

$$A(^{197}\text{Au}) = 220 \pm 10\ \text{G} \qquad A(^{13}\text{C}) = 80 \pm 10\ \text{G}$$

$$A(\text{H}_\alpha) = 25 \pm 5\ \text{G} \qquad A(\text{H}_\beta) = 50 \pm 10\ \text{G}$$

The larger proton coupling constant was assigned to the β proton in analogy with the vinyl radical.[19]

Irradiation of argon matrices showing the signals A, B, and C discussed above with visible light ($\lambda > 4000$ Å) for 10 min caused

(19) Cochran, E. L.; Adrian, F. J.; Bowers, V. A. *J. Chem. Phys.* **1964**, *40*, 213. See also ref 17.

Table II. g Tensors, ^{197}Au Hyperfine Coupling Tensors, and Other Hyperfine Coupling Tensors of Au Complexes Examined

complex	g tensor	^{197}Au hf tensor, MHz	other hf tensor, MHz
$H_2C{=}CH_2$ Au	$g_x = 1.946$ (2)	$A_x = 1725$ (2)	$A_x(^{13}C) = 0$ (10)
	$g_y = 1.978$ (2)	$A_y = 1772$ (2)	$A_y(^{13}C) = 50$ (3)
	$g_z = 1.782$ (2)	$A_z = 1726$ (2)	$A_z(^{13}C) = 0$ (10)
HC≡CH Au	$g_x = 1.977$ (2)	$A_x = 1845$ (2)	
	$g_y = 2.003$ (2)	$A_y = 1888$ (2)	
	$g_z = 1.856$ (2)	$A_z = 1844$ (2)	
$H_2C{=}CH_2$ Au $H_2C{=}CH_2$	$g_x = 1.984$ (2)	$A_x = 28$ (5)	$A_x(^{13}C) = 0$ (8)
	$g_y = 1.846$ (2)	$A_y = 103$ (2)	$A_y(^{13}C) = 52$ (3)
	$g_z = 2.180$ (2)	$A_z = 86$ (2)	$A_z(^{13}C) = 0$ (8)
H, C=OH, Au	$g = 2.002$ (6)	$A = 617$ (28)	$A(^{13}C\alpha) = 224$ (28)
			$A(H\alpha) = 70$ (14)
			$A(H\beta) = 140$ (28)

complete disappearance of the B signals, while the signals A and C remained unchanged. It is thus shown that the gold(0)–acetylene adduct of structure III is more stable than the gold(0)–acetylene complex of structure I.

Discussion

The **g** tensors and the hf coupling tensors of all the Au(0) complexes and adduct examined in the present study are compiled in Table II. The table incorporates the result of **g** tensor analyses (discussed below), which allowed determination of the orientations of the tensors relative to the respective molecular axes. As in structures I and II depicted earlier, the z axis is perpendicular to the molecular plane, while the x axis is parallel to the C–C bond(s). The coupling constants determined in G were converted to those in MHz by multiplication by $g_i\beta$.

As shown in our earlier study, the LCAO molecular orbitals of the dative bonds and the semifilled orbital of copper(0)–mono(ethylene) or copper(0)–mono(acetylene) may be given as in eq 3.[9] The first orbital represents the dative interaction between

$$\Phi_1 = a_1\phi_M(s) + b_1\phi_M(p_y) + c_1\pi_y \quad (3a)$$

$$\Phi_2 = a_2\phi_M(d_{xy}) + c_2\pi_y^* \quad (3b)$$

$$\Phi_3 = a_3\phi_M(s) - b_3\phi_M(p_y) + c_3\pi_y \quad (3c)$$

the filled π_y orbital of the ligand and a vacant sp_y orbital of the metal atom, the second orbital the interaction between the filled d_{xy} orbital of the metal atom and the vacant antibonding π_y^* orbital, and the third the semifilled orbital. The π_y orbital in Φ_3 is due to the orthogonality requirement.

In the cases of bis(ethylene) complexes of copper(0) and silver(0), and bis(acetylene)copper(0), the following dative bonds were envisaged:

$$\Phi_1 = a_1\phi_M(s) + (b_1/2^{1/2})(\pi_y - \pi_y') \quad (4a)$$

$$\Phi_2 = a_2\phi_M(p_y) + (b_2/2^{1/2})(\pi_y + \pi_y') \quad (4b)$$

$$\Phi_3 = a_3\phi_M(d_{xy}) + (b_3/2^{1/2})(\pi_y^* + \pi_y^{*\prime}) \quad (4c)$$

$$\Phi_4 = a_4\phi_M(p_x) + (b_4/2^{1/2})(\pi_y^* - \pi_y^{*\prime}) \quad (4d)$$

The first two orbitals represent dative interaction between the filled π_y orbitals of the two ligands and the vacant s and p_y orbitals of the metal atom, respectively. The last two orbitals represent dative interaction between the vacant antibonding π_y^* orbitals of the ligands and the filled d_{xy} and semifilled p_x orbitals of the metal atom.

The bonding schemes responsible for the formation of the gold(0)–mono(ethylene) and gold(0)–mono(acetylene) of structure I and that responsible for the formation of bis(ethylene)gold(0) must be similar to those of the corresponding complexes of the copper and silver atoms. The ESR spectra observed here from the Au(0) complexes of structure I and II must hence be compatible with the semifilled orbitals given by eq 3c and eq 4d, respectively.

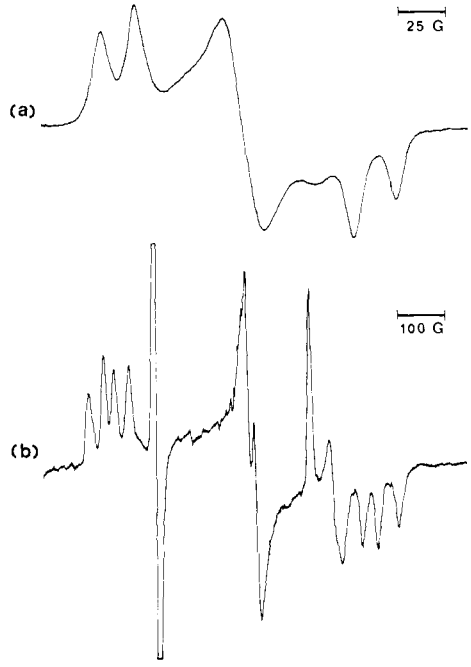

Figure 7. ESR spectra of (a) bis(ethylene)silver(0) and (b) bis(ethylene)gold(0). Note the difference in the field scales.

It has been shown that, for a radical having a nondegenerate ground state $|0\rangle$, deviation of the **g** tensor from the spin only value g_e (=2.0023) is given by eq 5.[20] Here i (= x, y, z) represents

$$g_i - g_e = -2\lambda\sum_n \frac{\langle 0|L_i|n\rangle\langle n|L_i|0\rangle}{E_n - E_0} \quad (5)$$

an axis of the principal **g** tensor, L_i the orbital angular momentum operator, and λ the one electron spin–orbit coupling constant. The summation is performed over all the excited states. In evaluating eq 5 in terms of LCAO–MO's, only one-centered integrals need to be retained, and for each atomic integral the spin–orbit coupling constant of the particular atom is chosen. The spin–orbit coupling constant of Au (evaluated from its $5d^{10}\,6p^1$ state)[12] is 2544 cm^{-1}, whereas that of carbon is only 15 cm^{-1}. It follows that the **g** tensor of the Au(0) complexes examined here would be determined essentially by the Au(p) orbital parts of eq 3c and eq 4d, respectively.

Recalling that the matrix element $\langle p_i|L_j|p_k\rangle$ would have nonvanishing value only when the indices i, j, and k are all different from each other, one can immediately state $g_y = g_e$ for gold(0)–mono(ethylene) and gold(0)–mono(acetylene), and $g_x = g_e$ for gold(0)–bis(ethylene).

For gold(0)–mono(ethylene) and gold(0)–mono(acetylene) all the molecular orbitals involving the Au($6p_x$) and Au($6p_z$) orbitals would be vacant ($E_n > E_0$). Furthermore there could exist a low-lying vacant MO consisting of Au($6p_x$) and π_y^* orbital of the ligand that could induce a large negative g shift. The g value showing the smallest deviation from g_e was hence identified as g_y, and the g value with the largest negative shift as g_z.

As for bis(ethylene)gold(0) the symmetry of the complex is such that little mixing is expected between the vacant Au($6p_z$) orbital and the ligand orbitals. On the other hand there exists a closely lying filled orbital ($E_n < E_o$) involving the Au($6p_y$) orbital and the π_y orbitals of the ligands as in eq 4b. Hence the g value showing a large negative shift was identified as g_y, and the g value with a large positive shift as g_z.

Figure 7 shows a comparison of the ESR spectrum of bis-

(20) Pryce, M. H. L. *Proc. Phys. Soc., London, Sect. A* **1950**, *63*, 25.

(ethylene)silver(0)[9] and that of bis(ethylene)gold(0). The close similarity of the two spectra is conspicuous. The magnetic field scale in the former is one-quarter of that in the latter. It is intriguing to realize that the spin–orbit coupling constant of Ag (=614 cm^{-1}) is also approximately one-quarter that of Au, and the similarity of the spectra revealed here must reflect the similarity in the bonding schemes and the resulting molecular orbitals of the two complexes. The ^{13}C isotopic substitution affected only the highest field component in the case of bis(ethylene)silver(0), also.[21]

The essential features of the hf coupling tensor to a magnetic nucleus is determined by the distribution of the unpaired electron in the vicinity of the nucleus. The ^{197}Au hf coupling tensors of the Au(0) complexes of structures I and II must therefore be approximately axially symmetric, the symmetry axis being parallel to the y axis for the former and being parallel to the x axis for the latter. The ^{13}C hf coupling tensors of these complexes would also be axially symmetric, the symmetry axis being parallel to the y axis in both cases. As seen in Table II all the ^{197}Au and ^{13}C hf coupling tensors of the complexes examined here are exactly or nearly axially symmetric, and the directions of the symmetry axes are exactly as predicted.

It has been shown that the principal elements, $A_\parallel$ and $A_\perp$, of an axially symmetric hf coupling tensor can be related to the isotropic term A_{iso} and the anisotropic term A_{dip} as follows:[16]

$$A_\parallel = A_{iso} + 2A_{dip} \tag{6a}$$

$$A_\perp = A_{iso} - A_{dip} \tag{6b}$$

where

$$A_{iso} = g_e\beta_e g_n\beta_n \frac{8\pi}{3}|\Phi(0)|^2$$

$$A_{dip} = g_e\beta_e g_n\beta_n\left\langle \frac{3\cos^2\theta - 1}{2r^3}\right\rangle = g_e\beta_e g_n\beta_n \frac{2}{5}\left\langle \frac{1}{r^3}\right\rangle_p$$

Here $|\Phi(0)|^2$ represents the spin density at the magnetic nucleus, r the separation between the unpaired electron and the magnetic nucleus, and θ the angle between r and the symmetry axis. Only a spin density in an s orbital contributes to A_{iso}, and that in a non-s orbital contributes to A_{dip}. The second expression for A_{dip} applies when a unit spin density is located in a p orbital of the magnetic nucleus.

Analyses of the observed Au hf coupling tensors of the monoethylene and monoacetylene complexes in terms of eq 6 yield for $Au(C_2H_4)$ A_{iso} = 1741 MHz and A_{dip} = 15 MHz, for $Au(C_2H_2)$ A_{iso} = 1859 MHz and A_{dip} = 14 MHz. It is illustrative to compare these values with A_{iso}^0 = 3138 MHz, the hf coupling constant of Au atoms ($6s^1$) isolated in an argon matrix, and A_{dip}^0 = 48 MHz, a value estimated for a unit spin density in the Au(6p) orbital from the known hf splitting term $a_{(j=1/2)}$ of the ^{205}Tl atoms ($6s^2\ 6p^1$).[22] We may thus conclude, for the semifilled orbitals of gold(0)–mono(ethylene) and gold(0)–mono(acetylene) given by eq 3c, $a_3^2 \simeq 0.57$ and $b_3^2 \simeq 0.30$.

Analysis of the ^{13}C hf coupling tensor determined for gold(0)–mono(ethylene) in terms of eq 6 yields the following: $A_{iso} \simeq A_{dip} \simeq 17$ MHz. These values may be compared with A_{iso}^0 = 3164 MHz and A_{dip}^0 = 92 MHz, the values theoretically estimated for a unit spin density in the C(2s) and C(2p) orbitals, respectively.[23] When the unpaired electron resides only in a non-s orbital of a magnetic nucleus, A_{iso} of a small magnitude is known to occur through polarization of filled, inner orbitals. The ^{13}C A_{iso} determined above is believed to be of this type. From the ^{13}C A_{dip} determined above one then obtains, neglecting all the overlap integrals, $c_3^2 \simeq 0.37$. The sum of these distributions ($a_3^2 + b_3^2 + c_3^2 = 1.24$) is substantially above unity; the result is considered reasonable, however, in view of the approximations involved.

Similar analyses of the ^{197}Au and ^{13}C hf coupling tensors determined for bis(ethylene)gold(0) in terms of eq 6 yield: for ^{197}Au, A_{iso} = −72 MHz and A_{dip} = 22 MHz; for ^{13}C, A_{iso} = 17 MHz and A_{dip} = 17 MHz. In the analysis of the Au hf tensor it was assumed $A_\parallel = A_x$ = −28 MHz and $A_\perp = (A_y + A_z)/2$ = −95 MHz. Small A_{iso}'s determined for both nuclei are attributed to polarization of filled inner orbitals. On the basis of A_{dip}^0's (48 MHz and 92 MHz) cited earlier for a unit spin density in the Au(6p) and C(2p) orbitals, we hence conclude, for the semifilled orbital of bis(ethylene)gold(0) given by eq 4d, $a_4^2 \simeq 0.46$ and $b_4^2 \simeq 0.74$. Again, though the sum of distributions exceeds unity, the result is considered reasonable in view of the approximations involved.

As stated earlier, when allowed to react in the vapor phase, Ag atoms and acetylene formed adducts of the vinyl form III.[9] The isotropic hf coupling constants oberved from the silver–acetylene and gold–acetylene adducts are compared below. The numbers

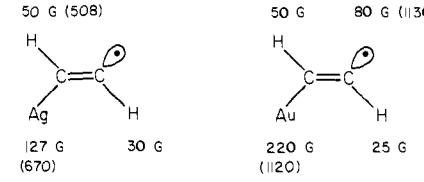

in parentheses are the coupling constants expected from a unit spin density in the H(1s), Ag(5s), Au(6s), and C(2s) orbitals, respectively.[14,23] The proximity of the spin density distributions in these radicals is apparent. However, unlike the silver–acetylene adduct, the gold–acetylene adduct formed spontaneously within the argon matrices when the acetylene concentration was above ~2%.

Rytter and Gruen reported, in their IR study of ethylene/argon matrices, preponderance of ethylene dimers in matrices with ethylene concentration above 2%.[24] It has also been shown that, in the Cu/acetylene/Ar system, bis(acetylene)copper(0) is the major product when the acetylene concentration is above 5%.[9] More recently evidence has been presented for the presence of acetylene dimers in the Na/acetylene/Ar system when the acetylene concentration is above ~2%.[25] For the ethylene dimer, a crossed arrangement whereby two ethylene molecules are held by weak, quadruple hydrogen bonding has been suggested. A staggered arrangement such as shown below would enable two acetylene molecules to couple through double hydrogen bonding.

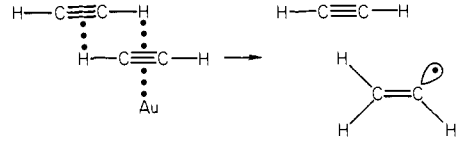

We believe the gold–acetylene adduct results from reaction between a gold atom and an acetylene dimer, the primary step being the dative interaction with one member of the dimer in the scheme of the monoligand complex. As stated earlier, Ag(0) and acetylene do not form a bona fide π-coordinated complex.

The EHT (extended Hückel theory) molecular orbital calculation places the bonding and antibonding π orbitals of ethylene at −13.2 and −8.2 eV, respectively.[26] The corresponding orbitals of acetylene are at −13.5 and −7.1 eV. Figure 8 compares schematically the π and π^* orbital levels of ethylene and the valence orbital levels of the Cu, Ag, and Au atoms.[12] The energy levels of copper(0)–mono(ethylene) and the dative interactions responsible for its formation are also indicated. The exact energy levels of the complex are not known; they are drawn in the figure to indicate their positions relative to the interacting orbitals.

On inspection of the figure one can immediately surmise that, in this series of metal–ligand combinations, dative interactions

(21) Kasai, P. H. *J. Phys. Chem.* **1982**, *86*, 3684.
(22) See, for example, Kopfermann, H. "Nuclear Moments"; Academic Press: New York, 1958; pp 123–138.
(23) Morton, J. R.; Preston, K. F. *J. Magn. Reson.* **1978**, *30*, 577.
(24) Rytter, E.; Gruen, D. M. *Spectrochim. Acta, Part A* **1979**, *35*, 199.
(25) Kasai, P. H. *J. Phys. Chem.* **1982**, *86*, 4092.
(26) Hoffman, R. *J. Chem. Phys.* **1963**, *39*, 1397.

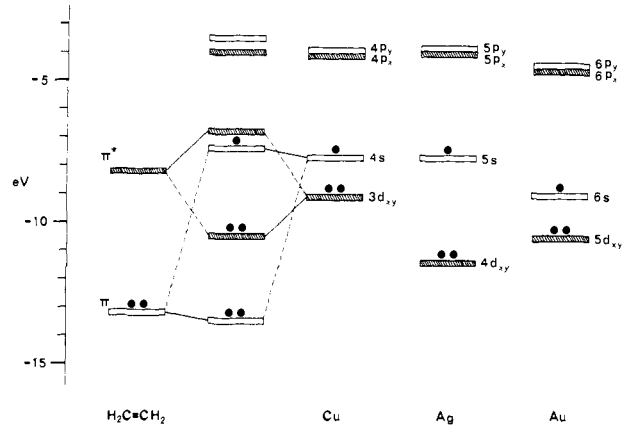

Figure 8. Energy level diagram showing the π and π^* orbitals of ethylene and the valence orbitals of the metal atoms (Cu, Ag, and Au) relevant to π-coordination. The energy levels of copper(0)-mono(ethylene) and the dative interactions responsible for its formation are also indicated.

between the filled π orbital(s) and the vacant s and/or p orbital of the metal atom (eq 3a, 4a, and 4b) are probably insignificant. Thus copper(0)-mono(ethylene) and copper(0)-mono(acetylene) are held primarily by the dative interaction between the d_{xy} and π^* orbitals (eq 3b). The corresponding Ag-monoligand complexes are not formed because of the larger separation between the d_{xy} and π^* orbitals. The formation of bis(ethylene)copper(0) and bis(acetylene)copper(0) is attributed to the dative bond between the d_{xy} and π^* orbitals (eq 4c) and to the one-electron dative bond between the p_x and π^* orbitals (eq 4d). Bis(ethylene)silver(0), on the other hand, is probably held only by the one-electron dative bond of eq 4d.

In a diligand complex of structure II the overlap between the p_x and π^* orbitals would be sensitive to the C-C bond length of the ligands. The shorter C-C bond length of acetylene must adversely affect this overlap; bis(acetylene)silver(0) is not formed. A similar situation has been encountered in the dative interaction between the Al atom ($3s^2,3p^1$) and ethylene and that between Al and acetylene.[27] Aluminum(0)-mono(ethylene) complex is known. Its formation is attributed to the one-electron dative bond between the Al($3p_x$) orbital parallel to the ligand and the π^* orbital of the ligand. The corresponding acetylene complex of Al(0) is not formed.

The complexing ability of the Au atoms is similar to that of Cu in that they can both make the monoligand complex with either ethylene or acetylene. It is similar to that of Ag, however, in that they can both make the diligand complex with ethylene, but not with acetylene.

Registry No. I (M = Au), 87136-54-7; III (M = Au), 84074-14-6; $Au(CaH_4)$, 61943-23-5; gold(0)-bis(ethylene), 87136-55-8; acetylene, 74-86-2.

(27) Kasai, P. H. *J. Am. Chem. Soc.* **1982**, *104*, 1167.

Communications to the Editor

Practical, Cobalt-Mediated, Diastereoselective Synthesis of the 11-(Trimethylsilyl)-3-methoxyestra-1,3,5(10),8(14),9(11)-pentaene Nucleus: A Novel Steroid Intermediate. First Observation of Hindered Rotation in a Vinyltrimethylsilane

Jean-Claude Clinet, Elisabet Duñach, and K. Peter C. Vollhardt*

Department of Chemistry
University of California, Berkeley
and the Materials and Molecular Research Division
Lawrence Berkeley Laboratory
Berkeley, California 94720

Received April 1, 1983

We have recently introduced cobalt-mediated intramolecular achiral enediyne [2 + 2 + 2] cycloadditions as a synthetic method in chiral polycyclic diene construction.[1] We have now found that chiral substrates A (Scheme I) may in some cases [e.g., R_1 = $Si(CH_3)_3$, R_2 = CH_3, $C_6H_5CH_2$, or CH_3OCH_2] undergo the same reaction with remarkable diastereoselectivity, out of the four possible products basically only B (major) and C (minor) being formed.[2]

These transformations may be regarded as suitable models for a diastereoselective synthesis of known and, more importantly, novel hitherto inaccessible steroids.[3] Retrosynthetic analysis of the problem suggests the disconnection **1** → **2**, the ether protecting group chosen such as to maximize the cis stereochemistry in the D ring of **1**.

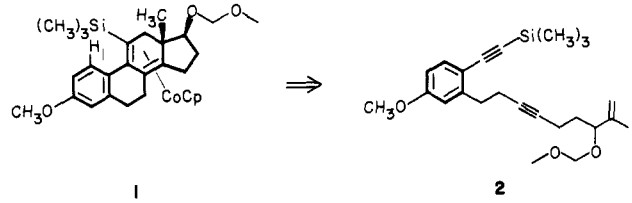

1 **2**

A convergent and efficient (42% overall yield) synthetic route to enediyne **2** is shown in Scheme II.[4] It has as its key features an oxazoline-directed ortho-lithiation, methylation, deprotonation sequence,[5] alkylation of the resulting benzyl anion with 6-chloro-4-hexynal ethylene acetal,[6,7] formolysis,[8] Grignard addition,

(1) (a) Sternberg, E. D.; Vollhardt, K. P. C. *J. Am. Chem. Soc.* **1980**, *102*, 4839; *J. Org. Chem.* **1982**, *47*, 3447. (b) Chang, C.; Francisco, C. G.; Gadek, T. R.; King, J. A., Jr.; Sternberg, E. D.; Vollhardt, K. P. C. In "Organic Syntheses: Today and Tomorrow"; Trost, B. M., Hutchinson, C. R., Eds.; Pergamon Press: New York, 1981; p 71. (c) Gadek, T. R.; Vollhardt, K. P. C. *Angew. Chem.* **1981**, *93*, 801; *Angew. Chem., Int. Ed. Engl.* **1981**, *20*, 802.

(2) Stereochemical assignments were based on ^1H NMR spectroscopic analysis,[1] two X-ray structural determinations (see supplementary material), and chemical correlation of ligands by oxidative demetalation.

(3) Akhrem, A. A.; Titov, Y. A. "Total Steroid Synthesis"; Plenum Press: New York, 1970. Blickenstaff, R. T.; Gosh, A. C.; Wolf, G. C. "Total Synthesis of Steroids"; Academic Press: New York, 1974. Lednicer, D. "Contraception: the Chemical Control of Fertility"; Marcel Dekker: New York, 1969.

(4) All new compounds were completely characterized (see ref 11) and gave satisfactory spectral and analytical data.

(5) Gschwend, H. W.; Hamdan, A. *J. Org. Chem.* **1975**, *40*, 2008; *Ibid.* **1982**, *47*, 3652.

(6) Prepared by alkylation of propargyl alcohol with 3-bromopropanal ethylene acetal[6] [$LiNH_2$, NH_3(l), 4 h, 90%; bp 85 °C (0.1 mm)], followed by chlorination [(a) CH_3SO_2Cl, CH_2Cl_2, $(CH_3CH_2)_3N$, -40 °C, 4 h, room temperature; (b) LiCl, DMF, 60 °C-room temperature, 12 h, 86%; bp 74 °C (0.8mm)].

(7) Büchi, G.; Wüest, H. *J. Org. Chem.* **1969**, *34*, 1122.

(8) Gorgues, A. *Bull. Soc. Chim. Fr.* **1974**, 529.

0002-7863/83/1505-6710$01.50/0